Consequences of Degraded Containment in a Severe Nuclear Power Plant Accident

Zachary Jankovsky, Christopher Jones, and Donald Kalinich

Sandia National Laboratories, 1515 Eubank Blvd. SE, Albuquerque, New Mexico, 87123
jankovsky.3@osu.edu

INTRODUCTION

The most common form of containment for nuclear power plants in the USA comprises a steel-lined concrete structure [1], in which the concrete and steel have a symbiotic relationship. The reinforced or pre-stressed concrete structure resists internal or external loading while the steel liner provides a leak-tight barrier to contain radionuclides in the event of an accident. If the liner has a pre-existing breach and a severe accident subsequently occurs, the concrete will contain the accident pressure until tensile cracks begin to form and release the internal pressure. Such liner degradation has been observed in plant inspections [2]. This paper examines a simple crack formation scheme added to a station blackout model, and compares the estimated radionuclide releases.

MODELING CONDITIONS

Accident Parameters

The severe accident under examination is a short-term station blackout (STSBO), in which all electric power, including batteries, is lost. This results in a loss of all active safety systems. Such a condition may result from a severe seismic event, and is described in the State-of-the-Art Reactor Consequences Analyses (SOARCA) report [3]. A model of the Surry power plant in Virginia is used in this study, as it was used as a representative PWR plant in the SOARCA study. Surry has a steel-lined reinforced concrete containment structure, with the containment volume kept at a sub-atmospheric pressure during normal operating conditions.

MELCOR is a system-level code used to simulate severe reactor accidents, from initiating condition to potential environmental release. MELCOR is developed at Sandia National Laboratories for the Nuclear Regulatory Commission, and is commonly used to evaluate accident scenarios for reactor licensing purposes. An existing MELCOR input deck modeled after the Surry plant under an STSBO condition from the SOARCA study was used as the base case for this analysis.

In the base MELCOR deck, there are two pathways for material to leave containment to the environment. The first is design leakage, which is limited to 0.1% of volume per day. The second represents containment failure due to overpressurization. The design pressure for the containment is 310 kPag (45 psig), and the containment failure pathway opens 676 kPag (98 psig). This pathway is disabled in the crack test cases, as it is similar in nature to the degradation under test.

Crack Formation

A small section of the steel liner is assumed to be compromised, possibly by foreign material or improper installation [2]. Within the compromised area a single crack is presumed to run through the entire depth of the concrete containment structure to the environment, with its width (W) dependent on the pressure differential between the two volumes, as in Eq. 1. W is the crack width in m, $P_{cont,g}$ is the gage pressure of containment in Pa, and $P_{init}(X)$ is the crack initiation pressure in Pa for X.

The crack initiation pressure was estimated from basic pressure vessel theory and an estimate of the tensile capacity of the reinforced concrete. The hoop stress is a function of the containment diameter and the internal pressure, while the tensile capacity of the concrete is estimated to be 10% of the compressive strength, estimated at 34,500 kPa. A precise value for the tensile capacity of the concrete could be obtained experimentally, however this was beyond the scope of this simple study. The crack initiation pressures (absolute) and growth slopes are given as Tables I and II, respectively. The format used for naming the experimental cases is X-Y, in which X is the crack initiation pressure and Y is the crack growth slope. These conditions are combined to create 9 cases. The length of the crack was varied for each crack growth slope to maintain an approximate crack aspect ratio, and is also given in Table II. The crack is assumed to be rectangular.

TABLE I. Crack Initiation Pressures Tested.

X	$P_{init}(kPa)$	$P_{init}(psi)$
1	267	38.7
2	308	44.7
3	350	50.7

$$\begin{cases} W = 0, & P_{cont,g} \leq P_{init}(X) \\ W = P_{cont,g}Y & P_{cont,g} > P_{init}(X) \end{cases} \quad (1)$$

TABLE II. Crack Growth Slopes, Lengths, & Hydraulic Diameters Tested.

Y	$Slope\ (m/kPa)$	$Length\ (m)$	$D_h\ (m)$
1	2.8e-08	0.0076	1.95e-05
2	2.8e-07	0.076	1.95e-04
3	2.8e-06	0.76	1.95e-03

Crack Flow Properties

The hydraulic diameter affects the Reynolds number, and thus the pressure loss in the flow. A constant value is required for each case because the hydraulic diameter of a flow path is not allowed to change during a MELCOR simulation. This is because flow paths in MELCOR typically represent set geometries such as pipes and valves. The hydraulic diameter is calculated at 345 kPag (50 psig). This intermediate pressure

was chosen by examining the base case, in which containment pressure is normally -34 kPag (-5 psig) and containment failure begins at 676 kPag (98 psig). The equation is taken from the MELCOR User's Guide [4]: "The conventional definition is given by 4 times the flow area divided by the wetted perimeter."

The viscosity of the escaping gas is assumed to match that of the main containment volume. The combined molar fractions of steam and air are at or above 89% of the containment atmosphere throughout the base case, and so the mixture is assumed to be a binary mixture of air and steam for viscosity calculation. The viscosity of the mixture is calculated using the Wilke formula [5], which takes into account the molar mass and mole fraction of each component. The viscosity of the mixture (steps omitted) is calculated as:

$$\mu = \frac{\mu_A}{\left(1 + \phi_{AS}\frac{\gamma_S}{\gamma_A}\right)} + \frac{\mu_S}{\left(1 + \phi_{SA}\frac{\gamma_A}{\gamma_S}\right)} \tag{2}$$

Where μ is the mixture viscosity in $kg/m*s$, μ_S is the steam viscosity, μ_A is the air viscosity, ϕ_{AS} is a unitless coefficient that represents the effect of air on the partial viscosity of steam, ϕ_{SA} is the effect of steam on the partial viscosity of air, γ_S is the mole fraction of steam in containment, and γ_A is the mole fraction of air. This method rapidly becomes cumbersome for multiple gases as the influence (ϕ_{ij}) of each gas i on each other gas j must be calculated. As a side study, a simplified method [6] of calculating viscosity was also tested.

$$\mu = \frac{\sum\left(\mu_i x_i \sqrt{M_i}\right)}{\sum\left(x_i \sqrt{M_i}\right)} \tag{3}$$

This method takes into account the individual viscosity of each gas (μ_i), its mass fraction (x_i), and its molar mass (M_i) in g/mol. Six gases were considered: water vapor, oxygen, nitrogen, hydrogen, carbon monoxide, and carbon dioxide. Individual gas viscosities were calculated using Sutherland's formula [7], with the exception of water vapor which was calculated using a formula from Wilke [5].

$$\mu_i = \mu_{0i}\frac{T_{0i} + C_i}{T + C_i}\left(\frac{T}{T_{0i}}\right)^{3/2} \tag{4}$$

Where μ_i is the individual gas viscosity in $kg/m*s$, μ_{0i} is the individual gas viscosity at the reference temperature, T_{0i} is the reference temperature in K, C_i is the Sutherland's constant, and T is the containment temperature. The two methods of determining viscosity are compared in Fig. 1. The simplified viscosity is higher than the Wilke viscosity at every time step, up to 15% higher at the point of hot leg nozzle failure and 8% higher on average. The effect on total mass of gas leakage (see Table III) was examined by re-calculating flow using the simplified viscosity, and it was found that the Suzuki formula was most sensitive, varying up to 3.5% from the original estimated mass leakage. Because the radionuclide release (Table IV) was taken directly from MELCOR, it is not affected by the method used to calculate viscosity.

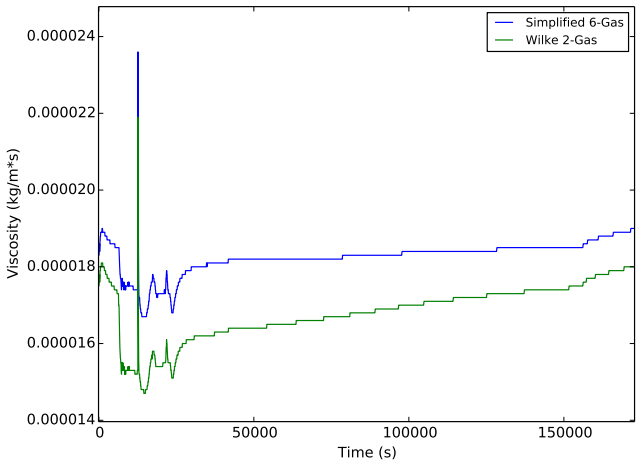

Fig. 1. Containment Viscosity vs Time.

Crack Flow Estimation

The mass flow rate through a flow path is automatically calculated by MELCOR. A calculation of the mass flow rate using empirical concrete crack flow formulas was also desired. The three formulas used were described and compared in Reference [8]. The following equation was developed by Rizkalla et al. [9] to calculate the volumetric flow rate through a crack:

$$Q = \frac{L}{P_2}\left(\frac{P_1^2 - P_2^2}{t\frac{k^n}{2}\left(\frac{\mu}{2}\right)^n \frac{(R_M T)^{n-1}}{W^3}}\right)^{\frac{1}{2-n}} \tag{5}$$

$$n = \frac{0.133}{W^{0.243}} \tag{6}$$

$$k = \left(2.907 * 10^7\right) W^{1.284} \tag{7}$$

Where Q is the volumetric flow rate in m^3/s, L is the crack length in m, P_1 is the containment pressure in Pa, P_2 is the environment pressure in Pa, t is the crack depth in m, R_M is the specific gas constant of the mixture in $J/kg*K$, T is the containment temperature in K, and W is the crack width in m. The Rizkalla formula becomes numerically unstable as n approaches a value of 2. This occurred in the cases with the slowest crack growth rate (Y=1). The Nagano formula [10] was also used as an alternative to calculate volumetric flow through the crack and is given as Eq. 8. It is significantly simpler than the Rizkalla formula, and does not experience numerical instability. The Suzuki formula [11] was also used to calculate the volumetric flow rate, and is given as Eq. 9.

$$Q = LW^3\frac{P_1 - P_2}{12\mu t} \tag{8}$$

$$Q = 15.3W + (7.56 * 10^{-3})LW^3\frac{P_1 - P_2}{\mu t} \tag{9}$$

RESULTS AND ANALYSIS

The MELCOR model for the accident had a duration of 48 hours, and the crack parameters did not significantly change the course of the accident. At approximately 6,000 s the surge tank rupture disks fail, opening a path from the primary system to containment. At approximately 10,000 s, cladding failure begins and fission products are released into the primary system. At approximately 12,000 s in each case a hot leg nozzle failed, causing a spike in pressure and steam content of containment.

Over the rest of the scenario, the pressure (Fig. 2) and temperature (Fig. 3) of containment generally increase as more of the primary cooling system water is transferred to containment. A significant difference in system pressure can be seen for cases of Y=3. The crack area increases by a factor of 100 with each 10-fold step in growth slope, allowing substantially more leakage as the slope increases. The earliest crack opened at 19,680 s, and the latest at 30,240 s.

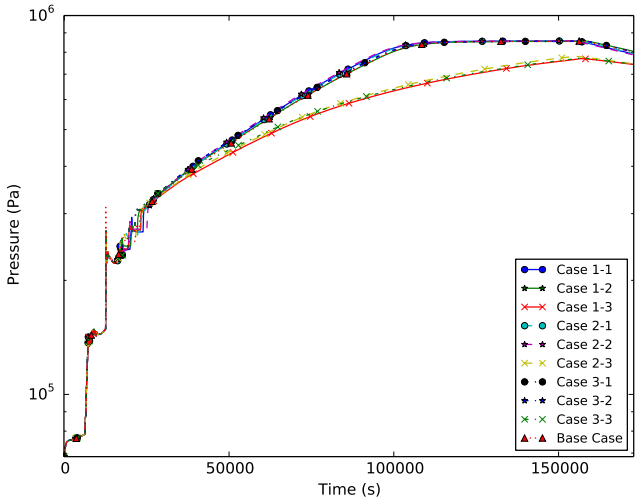

Fig. 2. Containment Pressure vs Time.

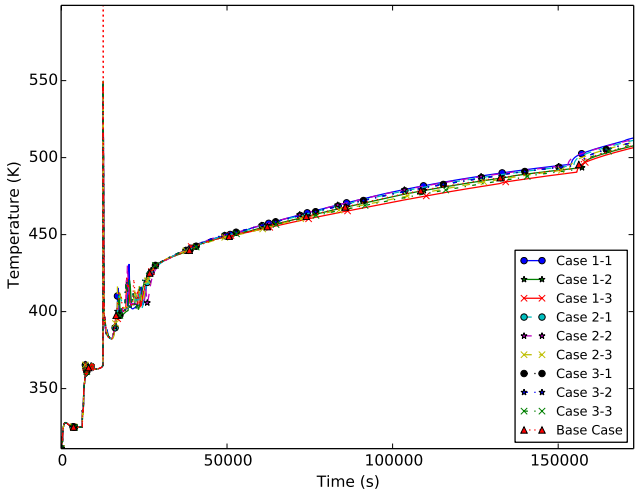

Fig. 3. Containment Temperature vs Time.

The mass flow rate returned by MELCOR for the crack is plotted on a semilog scale as Fig. 4. Only the MELCOR-calculated mass rate is given, as it is the only method of leakage calculation available for the base case. As expected, scenarios with similar crack growth slopes converge on the same leakage rate after opening. Because the containment failure flow path in the base case opens at 676 kPag (98 psig), it is not a factor until later in the accident. Once it is open it quickly jumps to a flow rate near that of the highest crack growth slope (Y=3).

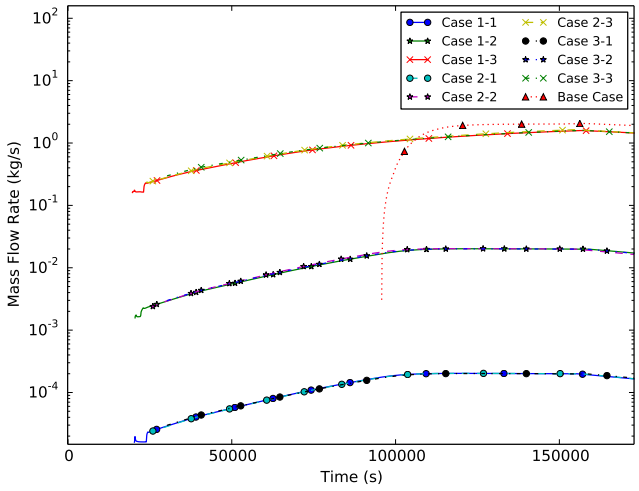

Fig. 4. Crack Flow Rate, MELCOR.

At n=2 for the Rizkalla formula, the flow rate diverges to infinity. All cases with the slowest crack growth rate (Y=1) experienced crack widths that resulted in the case crossing n=2, and were excluded from the analysis. The six remaining cases are multiplied by the density of the containment gas to obtain a mass flow rate. The flow rates returned by the Nagano & Suzuki formulas are also multiplied by density to obtain mass flow rates.

In order to compare total predicted gas release, the mass flow rates were integrated using the trapezoidal method (Eq. 10), where y_{n+1} is the cumulative release in kg at time step $n+1$, y_n is the cumulative release at time step n, t_{n+1} is the time at time step $n+1$, t_n is the time at time step n, x_{n+1} is the mass flow rate in kg/s at time step $n+1$, and x_n is the mass flow rate at time step n. The cumulative release throughout the accident according to the MELCOR mass flow calculation is given in Fig. 5. The final release for each case is given in Table III. The final release for the base case through the containment failure flow path as tabulated by MELCOR is given for comparison.

$$y_{n+1} = y_n + \frac{t_{n+1} - t_n}{2}(x_{n+1} + x_n) \tag{10}$$

Among the crack flow formulas, the closest agreement exists for the highest crack growth rate (Y=3). In these cases, the maximum and minimum values differ by a factor of about 60. For the medium crack growth rate (Y=2), the difference is a factor of 75. For the slowest crack growth rate (Y=1) the difference is a factor of 10,000.

The final radionuclide mass release fractions to the environment for each case are estimated by MELCOR and are shown in Table IV. The MELCOR chemical classes included

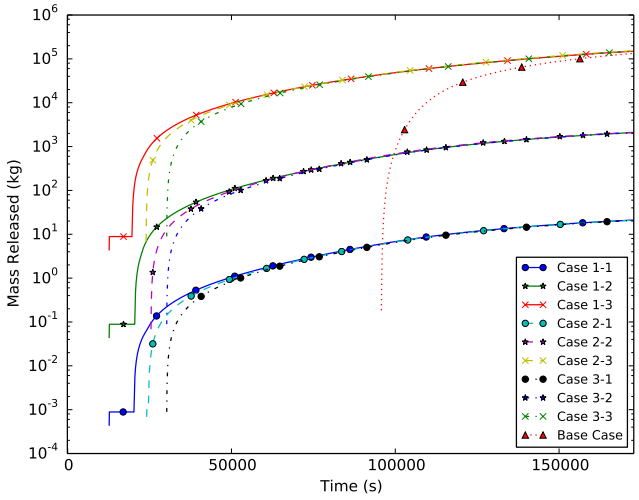

Fig. 5. Integrated Crack Flow Rate, MELCOR.

in the first column are: Xe, Cs, Ba, I, Te, Ru, Mo, Ce, and La [4]. Because xenon is the dominant release by mass, the release fractions are tabulated again without xenon. The ratio Z, which is the ratio of mass release from the case in question to the base case, is also included. The ratio Z was equal to or greater than 1 in each test case. It can be seen that the cases with the highest crack growth slope lead to the highest release of radionuclides.

TABLE III. Integrated Crack Flow Rate (kg).

Case	*MELCOR*	*Rizkalla*	*Nagano*	*Suzuki*
1-1	2.10e+01	∞	2.10e-01	2.10e-03
1-2	2.10e+03	1.00e+03	2.10e+03	2.80e+01
1-3	1.50e+05	4.20e+06	8.90e+06	4.30e+05
2-1	2.10e+01	∞	2.10e-01	2.10e-03
2-2	2.10e+03	1.00e+03	2.10e+03	2.90e+01
2-3	1.50e+05	4.50e+06	9.40e+06	4.60e+05
3-1	2.10e+01	∞	2.10e-01	2.10e-03
3-2	2.10e+03	1.00e+03	2.10e+03	2.80e+01
3-3	1.50e+05	4.40e+06	9.20e+06	4.40e+05
Base	1.34e+05	N/A	N/A	N/A

TABLE IV. Final Radionuclide Release Fractions.

Case	*All*	*No Xe*	*Z (All)*	*Z (No Xe)*
1-1	6.91%	0.013%	1.06	1.12
1-2	6.52%	0.015%	1.00	1.29
1-3	8.45%	0.202%	1.30	17.1
2-1	6.84%	0.015%	1.05	1.23
2-2	7.00%	0.014%	1.07	1.15
2-3	8.46%	0.127%	1.30	10.7
3-1	6.60%	0.017%	1.01	1.41
3-2	6.62%	0.018%	1.02	1.52
3-3	8.32%	0.127%	1.28	10.7
Base	6.52%	0.012%	N/A	N/A

CONCLUSIONS

The vast majority of radioactive material mass released to the environment was xenon released by cladding failure. The crack initiating pressure had no consistent effect on radioactive mass release, as the mass of xenon in containment was relatively stable by the time any of the cracks opened. The largest crack growth slope consistently led to the largest radionuclide release, while the 2 smaller growth slopes did not have a clear relationship in their releases. That the ratio Z was greater than or equal to 1 in each case is not unexpected because the built-in containment failure flow path is of a similar area of the high-slope cracks but opens at 676 kPag, while the modeled cracks open and begin releasing material much earlier in the accident.

The wide range of predicted overall mass release was not unexpected, as at a differential pressure as low as 2 psi the empirical formulas used can vary by multiple orders of magnitude [8]. The lack of very high pressure concrete cracking experiments may be a hindrance to numerical agreement: the experiments used to develop the formulas tested to less than 40 psi differential, while this accident peaks near a 110 psi differential.

REFERENCES

1. "Containment Integrity Research at Sandia National Laboratories," Tech. Rep. NUREG/CR-6906, Nuclear Regulatory Commission (2006).
2. "Containment Building Liner Corrosion - Corrosion and Leak Rate Models," Tech. Rep. ML13204A004, Nuclear Regulatory Commission (2013).
3. "State-of-the-Art Reactor Consequence Analyses (SOARCA) Report," Tech. Rep. NUREG-1935, Nuclear Regulatory Commission (2012).
4. "MELCOR Computer Code Manuals: Primer and User's Guide," Tech. Rep. NUREG/CR-6119, Nuclear Regulatory Commission (2000).
5. J. KNUDSEN, "Properties of Air-Steam Mixtures Containing Small Amounts of Iodine," Tech. Rep. BNWL-1326, Pacific Northwest Laboratory (1970).
6. T. DAVIDSON, "A Simple and Accurate Method for Calculating Viscosity of Gaseous Mixtures," Tech. Rep. Report of Investigations 9456, United States Department of the Interior (1993).
7. W. SUTHERLAND, "The viscosity of gases and molecular force," *Philosophical Magazine*, **5, 36**, 507–531 (1893).
8. T. WANG, "Gas Leakage Rate through Reinforced Concrete Shear Walls: Numerical Study," *Nuc. Eng. and Design*, **235**, 2246–2260 (2010).
9. S. RIZKALLA, "Air Leakage Characteristics in Reinforced Concrete," *ASCE Jnl. of Struct. Eng.*, **26**, 1149–1162 (1984).
10. T. NAGANO, "Experimental Study of Leakage through Residual Shear Cracks on R/C Walls," *Trans. 10th Intl. Conf. on Struct. Mech. in Reactor Tech* (1989).
11. T. SUZUKI, "Leakage of Gas through Cracked Concrete Walls," *Nuc. Eng. and Design*, **133**, 121–130 (1992).